UNIVERSITY OF WEST ATTICA

eISSN:3136-7658

Applied Manufacturing Intelligence Journal

Vol. 5, No. 1, January, 2026



Hoisting Path Optimization for Prefabricated Components Using a Causal-Guided Fusion TiDE-GNN Model

Konrad Wesołowski[1,*], Fabian Kołodziej[1], Radek Gromek[1]

[1] *Faculty of Electrical and Automatic Control Engineering, Czestochowa University of Technology, Czestochowa, 42-200, Poland*

Received 24 October 2025; Revised 08 January 2026; Accepted 13 January 2026; Published 17 January 2026

Abstract

Because path feasibility is jointly determined by tower-crane reach, component weight, temporary storage, weather disruption, barrier movement, installation sequence, and surrounding construction activities, causal-guided graph learning is used to optimise hoisting paths for prefabricated components under dense site constraints. This work aims to build a TiDE-GNN model that can convert multi-source hoisting records into a risk-aware path decision, in contrast to a shortest-distance suggestion. 1,420 prefabricated components, 18,600 potential paths, 9 tower-crane operation zones, 36 installation areas, and 6 risk-region classifications make up the simulated dataset. Utilise a TiDE temporal encoder to record path-condition changes during lifting windows, model the components, cranes, barriers, weather, route nodes, and installation targets as a dynamic graph, and apply causal-guided fusion to lessen spurious dependence on background correlations like component weight or repeated storage positions. The experiment shows that the suggested model has a lower average route cost than traditional graph neural scoring, A* search, genetic planning, and rule-based BIM checking. The warning accuracy is now 91.2%, the near-collision frequency has decreased to 5.4%, and each candidate group's median inference latency is still 0.42 seconds. According to ablation results, there is a decrease in the safety discriminating of temporary barrier regions and an increase in needless route warnings in the absence of causal fusion. TiDE-GNN may enhance the hoisting path's efficiency and safety, assist prefabricated construction lifting decisions, and offer comprehensible route evidence for planner approval and human inspection.

Keywords: Causal-Guided Graph Learning, Prefabricated Component Hoisting, TiDE-GNN Path Optimization, Tower Crane Scheduling, Risk-Aware Decision Support

1. Introduction

Heavy components must frequently be moved across storage yards, temporary routes, tower-crane working radii, and installation faces in prefabricated construction. Artificial intelligence research in construction engineering shows that these operations increasingly depend on structured data rather than isolated human judgment [1]. Hoisting-path planning is difficult because component mobility is shaped by dynamic site layout. Prefabricated-component layout research shows that storage position, passage occupancy, and installation sequence interact during daily production [2]. Crane-lift route studies further show that blind-lift zones, turning radius, and vertical transport must be considered together [3], while digital-twin hoisting management requires continuous links among field constraints, equipment state, and component information [4].

Current hoisting planning technologies often incorporate static site maps, operator experience, and rule verification. By including collision rules into a three-dimensional construction model, BIM-based tower-crane planning [5]

* Corresponding author: konrad.we@pcz.edu.pl

https://doi.org/10.68406/amij.2026.vol5iss1np3:30-41

➢ This is an open access article under the CC BY-NC-SA 4.0 license (https://creativecommons.org/licenses/by/4.0/).

© Authors retain all copyrights.

enhances geometric inspection; nevertheless, field circumstances could change faster than the model update cycle. The shipping, storage, lifting, and installation phases constitute an interconnected chain, and a delayed component or a blocked route might impact several following lifts, according to management studies of prefabricated building [6]. When risk variables are causally related, scheduling optimisation using genetic algorithms [7] can lower the total delay, but it does not explain why one potential option is safer than another. While ensemble learning-based construction safety assessment [8] offers high warning capabilities, standard feature vectors frequently miss the connection between the real source of risk and lifting activities. At an active site, a route selection is determined with incomplete information. Planners are aware of the scheduled crane schedule, but they are unaware of the precise moment a truck will depart the storage yard. Similarly, they are aware of the wind speed record, but they are unaware of the local gust between two building faces.

Data-driven hoisting optimisation should consider visual site perception, crane-state sequences, component properties, meteorological data and manually verified near-misses. Crane-lift automation research proposes moving from independent collision avoidance to semi-automatic operation decision support [9]. Construction monitoring can obtain local field conditions [10], and collision-free path planning supports route generation based on environmental geometry [11]. Point-cloud-based lift planning can also provide spatial evidence of temporary barriers, storage boundaries and feasible lifting corridors [12]. A learned model can also find spurious correlations. For example, a large component in a core-tube region may often have a restricted path, but the weight of the component alone does not pose a danger. Thus, a causal-guided model is required to learn large-scale trajectories and distinguish between direct safety factors and background correlations.

A Causal-Guided Fusion TiDE-GNN model for prefabricated-component hoisting path optimisation is developed in this work. Hoisting planning, graph-based construction optimisation, temporal sequence modelling, and causal decision support are reviewed in Section 2. The dynamic hoisting graph, causal fusion method, TiDE temporal encoder, graph message-passing layer, and path scoring target are all introduced in Section 3. Simulated experiments, including dataset statistics, baseline comparisons, ablation findings, robustness testing, runtime behaviour, and deployment-oriented review analysis, are reported in Section 4. This paper's conclusion, Section 5, summarises the key findings and shortcomings.

2. Related Work

2.1. Prefabricated Construction Hoisting Planning

Component storage, lifting order, crane selection, rigging conditions, installation tolerance, and safety-zone control are all included in hoisting planning for prefabrication construction. Component knowledge may be arranged before to manufacture and assembly to connect design data with lifting limitations, according to ontology-based DfMA research [13]. Prefabricated parts should be seen as a component of a housing-production system rather than as separate loads, according to modular building optimisation [14]. Construction safety supervision employing machine learning [15] has suggested enhancing the warning layer by identifying field states, and BIM-based safety planning [16] can detect hidden construction dangers beforehand. While the deployment of a data-rich representation has been supported by the research, the issue of choosing a safe and effective approach when several temporary restrictions change during the same lifting window has not been thoroughly addressed. Another issue is how to link real-time route evidence with design-level component information. Both the intended lifting sequence and whether the route is still physically accessible at the time of the lift must be known by a planning model.

2.2. Causal Fusion and Graph-Based Construction Optimization

Hoisting activities may be represented using graph modelling, and there are clear linkages between components, cranes, storage yards, barriers, installation locations, and warning zones. Message transmission can maintain node and edge interactions, which are necessary for the transfer of risk among several linked building objects, according to a general graph neural network study [17]. Reviews of graph neural network applications [18] have also demonstrated that local and global context may be included into graph learning without reducing the scene to independent variables. Route congestion following a peak in material delivery is one example of a delayed impact that may be included in effective long-sequence forecasting of time-dependent construction operations [19]. Because hoisting choices must have both high prediction accuracy and a clear connection between time-varying inputs and the end plan, interpretable temporal forecasting [20] is also important. Because a single component may be associated with several things at once, such as its storage rack, chosen crane, temporary transit corridor, adjacent façade, and installation target, a graph representation is especially useful for crane operations. These variables can be stored in a flat table, but an intelligible representation of the risk distribution among them is not possible.

2.3. Learning-Based Decision Support for Site Operations

Multi-source reasoning has replaced single-indicator prediction in learning-based decision support. Graph WaveNet research [21] illustrates that adaptive spatial dependencies may be learnt when fixed neighbourhoods are unsuitable, while spatiotemporal graph convolution [22] reveals how to concurrently describe spatial structure and temporal changes. Structure-learning and causal-discovery studies [23] have investigated how directed dependencies may be used to streamline the audit of model behaviour, while causal inference surveys [24] have offered a basis for distinguishing intervention-related features from spurious correlations. This means that while optimising a lifting path, the model should not only produce a path score but also explain the reasons behind it, such as closeness to objects, crane-radius overlap, wind disruption, poor sight, or sequencing pressure. This is not a forecasting issue. The planner must determine whether to approve, redesign, postpone, or forward the route to a senior operator; all of these decisions require verifiable proof.

3. Methodology

3.1. System Workflow and Data Representation

The system arranges lifting activities into shared decision windows. The simulated site contains 1,420 prefabricated components, including wall panels, beams, slabs, stair modules, balcony units, and facade panels, with 36 installation areas and 12 storage areas. Candidate-path selection depends on crane base position, hook-height sequence, slewing angle, load state, obstacle map, weather information, and schedule priority. Figure 1 shows the site-sensing and path-approval workflow. component data, crane telemetry, obstacle information, weather, and construction sequence are synchronized before causal fusion and graph learning are applied.

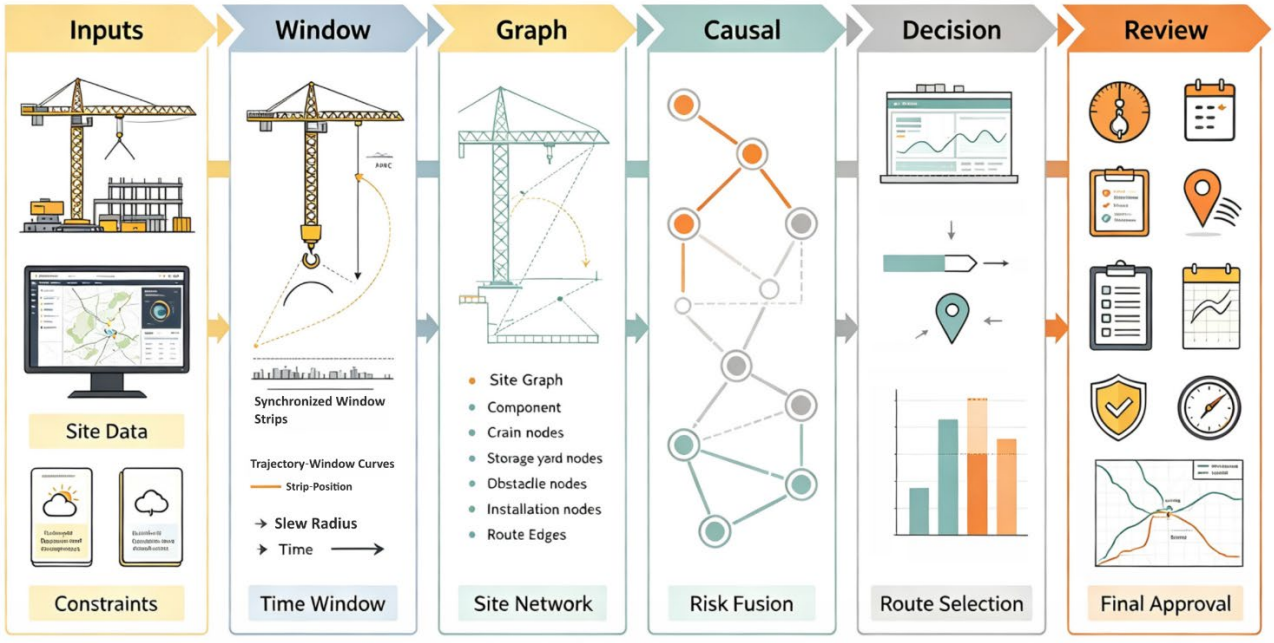


Figure 1. Causal-guided TiDE-GNN hoisting-path optimization workflow.

A dynamic graph is used to depict a hoisting scene. Weight, size, center of mass, lifting points, intended installation area, and permitted swing margin are all characteristics of component nodes. The operating radius, hook height, rated load, slewing angle, and occupied time window are all recorded by crane nodes. Scaffolds, temporary vehicles, piled materials, protected edges, other crane enclosures, and so on are examples of obstacle nodes. The graph additionally includes nodes for scheduling and weather; variations in visibility, wind speed, and installation priority might alter the danger rating of the same geometric path. In order for the model to evaluate a path's acceptability during planning rather than only after offline simulation, the state vector is tiny.

$$s_t = [x_c, x_q, x_o, x_w, x_p] \tag{1}$$

At time step t, the path-state vector contains component attributes, weather, obstacle context, crane status, candidate-path characteristics, and schedule information. Seventy percent of the 18,600 candidate paths are used for training, 10% for validation, and 20% for testing. The split is scenario-aware: storage-zone, tower-crane, and installation-floor groups are separated so that the model cannot repeatedly learn the same path for the same building face. Each path is labeled as permitted lift, near-miss, schedule delay, wind-sensitive operation, or manual review.

$$e_{ij} = \phi(v_i, v_j, d_{ij}, r_{ij}) \tag{2}$$

The relationship between two site elements is represented as an edge expression. Distance, relation type, time overlap, working-area interaction, and visibility are included. A graph is preferable to a flat feature table because it records which component is connected to the crane lifting it, which barriers it will face, and which installation target it is moving toward. This structure is useful because not every risk is visible at one point. A wall panel may be safe in an open area but dangerous when it passes through a crane-overlap region during strong wind.

3.2. Causal-Guided Fusion and TiDE Temporal Encoding

A causal-guided fusion layer is used to reduce misleading correlations. Many construction features are correlated because of scheduling rather than physical danger. Hard-to-install areas may be associated with busy storage zones, and heavier components may be lifted earlier in the day. The causal mask is created from expert rules, simulated interventions, and historical near-miss data. The mask changes the weight of selected features in the risk function instead of deleting learned characteristics, so useful context is retained while direct safety factors receive greater influence.

$$a_{ij} = \text{sigmoid}\left(w_c z_{ij} + b_c\right) \tag{3}$$

For path scoring, causal weight establishes how strongly two nodes in the graph are related to one another. Related factors including wind-to-swing sensitivity, path-to-obstacle clearance, and component-to-crane load ratio are given greater weights. If the indirect relationship—such as component category or popular storage area—does not immediately signal the path hazard, keep it but give it less weight. As a result, the issue of often occurring but low-risk patterns controlling the score will be eliminated as the model may be trained using the site's data.

$$h_t = \text{TiDE}(x_{t-L:t}) \tag{4}$$

After obtaining a candidate path from recent lifting history, TiDE scores the path using updated crane status, local obstacle information, material arrival, and weather evidence from the previous half hour. A compact temporal encoder is used because planning would be too slow with a large sequence Transformer. Figure 2 displays the process from multi-source input to temporal encoding, causal fusion, graph message passing, path scoring, and review output.

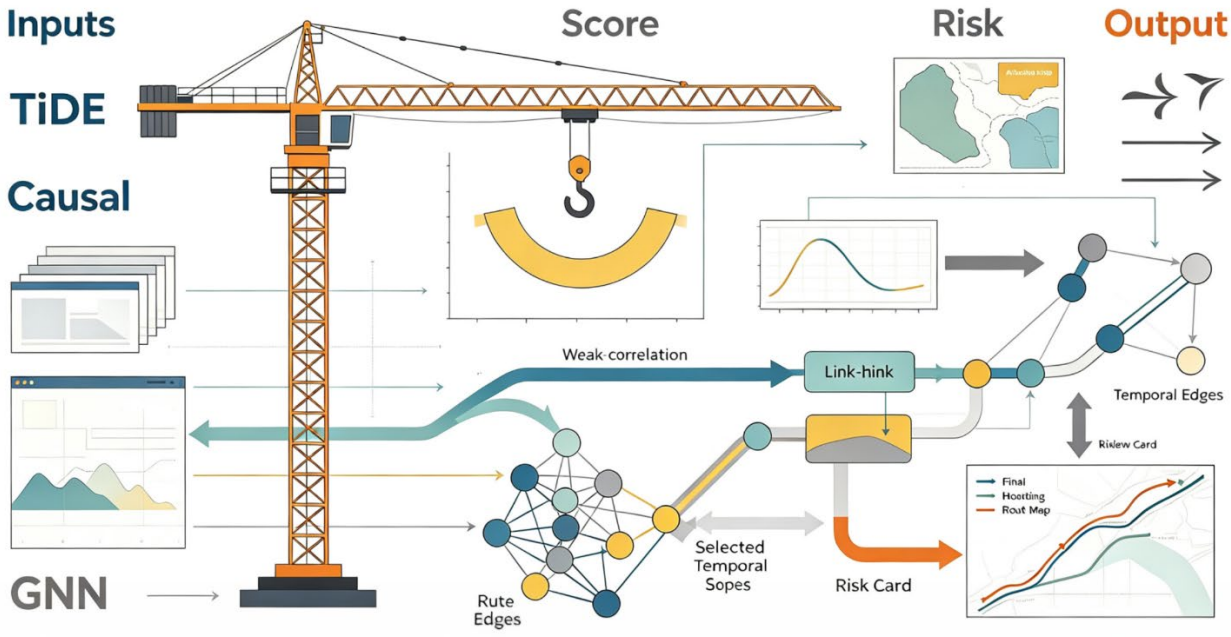


Figure 2. TiDE-GNN model structure with causal fusion and path-risk scoring.

To update a node, graph message transmission collects causally-weighted data from nearby nodes. The upgrade can address the issue of multi-hop risk; for instance, the crane will have to wait longer and lose some overlap time with another tower crane if a delivery vehicle blocks the warehouse's exit. As a result, the model considers that a path's risk is not a fixed-distance value but rather the outcome of related site characteristics.

$$h_i' = \sigma\left(W h_i + \sum a_{ij} W_g h_j\right) \tag{5}$$

3.3. Hoisting Path Scoring and Optimization Objective

The path score contains three components. Safety cost includes collision clearance, crane-load ratio, wind-sensitive swing, visibility, and protected-zone crossing. Efficiency cost includes travel distance, slewing effort, waiting time, and scheduling delay. Review demand is triggered when the model detects ambiguity or conflicting evidence, such as a

path with low geometric risk but high wind sensitivity. Missing evidence should not force a binary safe-or-unsafe decision; instead, it should increase the need for operator confirmation.

$$R(P) = \alpha C_{\text{safe}} + \beta C_{\text{time}} + \gamma C_{\text{review}} \tag{6}$$

The optimization objective selects the candidate path that satisfies strict safety constraints and has the lowest overall cost. A route is invalid if it exceeds rated load, violates minimum clearance, crosses a prohibited zone, or conflicts with crane-overlap rules. When several paths satisfy the hard constraints, the learned score chooses the route with better safety-efficiency balance. The objective must remain short enough for deployment because route updates may be required when a new obstacle, crane reservation, or weather change appears.

$$P^* = \underset{P \propto \Omega_{\text{safe}}}{\operatorname{argmin}} R(P) \tag{7}$$

A suggested route, risk score, list of causative evidence, and review label are all returned by the system. Normal approval, operator confirmation, delayed lift, and route redesign are the review labels. 64.8% of the lines in the simulated experiment had regular approvals, 18.7% needed operator confirmation, 9.5% were delayed, and 7.0% required route revision. The experimental discussion in the next section is based on these values.



Figure 3. Hoisting scenario composition and path-condition statistics. (a) Component-type distribution. (b) Hoisting-distance intervals. (c) Obstacle-zone categories. (d) Weather and visibility states.

4. Results and Discussion

4.1. Dataset Structure and Hoisting Scenario Distribution

Using nine tower-crane operating zones and 1,420 prefabricated components, the dataset produced 18,600 possible pathways. The path-condition statistics and scenario composition are shown in Figure 3. The component-type distribution is shown in Figure 3(a), with wall panels and slabs occupying the biggest shares due to their frequent horizontal transfer prior to vertical lifting and their recurring appearance throughout floors. Because of this distribution, the model cannot be evaluated just on the basis of uncommon heavy components; it must be able to manage regular, everyday lifts while also identifying the smaller set of complicated components that provide a significant danger to safety. The hoisting-distance intervals are displayed in Figure 3(b), which demonstrates that medium-distance pathways are the most prevalent; long-distance paths are comparatively uncommon but are more likely to cross temporary vehicle lanes and storage exits. Certain short pathways may go via crane-overlap regions or small installation gaps; therefore, they are not always safer. The obstacle-zone category split for moving equipment, temporary barriers, and immovable obstacles is shown in Figure 3(c). The two are not the same; transitory impediments must be detected by field sensing and promptly reassessed, whereas BIM can manage permanent obstructions. The weather and visibility state are depicted in Figure 3(d), thus in calm, windy, or low-visibility situations, the same path shape may have various safety implications. Additionally, the image illustrates the instability of a single cost weight. Lifting inertia is affected by component type, exposure time is altered by distance, clearance requirement is altered by obstructions, and swing sensitivity is altered by weather. Geometry, time, and risk causation must all be concurrently addressed in the distribution model.

The simulated evaluation's numerical setup is displayed in Table 1. To improve the transparency of the model performance discussion, provide the data scale, path count, risk labels, and evaluation split. Additionally, the chart demonstrates that the dataset is not balanced by design, with low-risk pathways occurring more frequently and route-redesign instances occurring less frequently but having a greater technical impact. The imbalance is intentional; only a small number of high-pressure lifts need strict safety monitoring, whereas the majority of real hoisting operations are regular lifts. As a result, the assessment will concurrently report warning accuracy, near-collision frequency, path cost, review effort, and delay. Additionally, Numerical Arrangement makes a distinction between parameters at the equipment and route levels. Installation regions are spatial transfers, weather windows are temporal disruptions, crane zones demonstrate equipment interaction, candidate pathways represent planning complexity, and component numbers indicate manufacturing size. As a result, the evaluation won't be predicated on just one element, such path length. Because infrequent but dangerous occurrences shouldn't be disregarded because of a limited sample size, a powerful anomaly-detection review [25] is appropriate in this situation.

Table 1. Numerical setup of simulated hoisting-path evaluation.

Item	Value	Main Classes	Risk Share	Use
Components	1,420	6 types	7.0% redesign	Path generation
Candidate paths	18,600	4 review labels	16.5% high risk	Training/test
Crane zones	9	Radius groups	11.2% overlap	Constraint check
Installation areas	36	Floor/face groups	9.8% delay	Scenario split
Weather windows	2,480	Wind/visibility	13.6% sensitive	Robustness

Additionally, scenario division will alter the problem's level of difficulty. The model must determine the risk based on structural connections rather than memorised path IDs if the test set includes a storage yard or installation face that was not observed during training. This is more in line with actual prefabricated building, and following site adjustments, the crane position, unloading timetable, and temporary barrier may all vary. Repeated pathways from the same level in a random split may give the impression that the learning challenge is simpler than it actually is since the model would encounter almost identical obstacle configurations and crane angles. The model must transition from known component-route relationships to unknown combinations in order to perform scenario-aware splitting. Additionally, it can demonstrate if the path score is associated with the real limitations or only with the statistical identification of a well-known lifting zone. The model cannot reuse a prior route label and must recalculate the risk based on component size, crane reach, and obstacle connections when a route from a new storage location reaches a known installation face. Frequent local patterns won't be enough to manage direct risk linkages like clearance and crane-radius conflicts; a causal fusion layer will still be needed.

The collection also includes operation and warning labels. Because speed reduction or operator confirmation may be added after the operation starts, a path may be deemed viable even if it has a relatively high risk. On the other hand,

if the tower crane timetable clashes with another lift, a path may have a low collision chance but still need a delay. As a result, the model is not employed as a stand-alone classifier but rather as a planning tool. Because planners typically analyse several flawed possibilities rather than looking for a single theoretically best solution, this design will bring the warning output more in line with site work. It will be handled differently as an error. While a missed route-redesign instance might lead to a high-consequence lifting dispute, a false alert raises coordination costs. As a result, the assessment will take into account the route cost, violation ratio, and review effort independently rather than combining all of the findings into a single accuracy figure.

4.2. Path Optimization Performance and Safety Comparison

The proposed approach is compared with A* search, genetic planning, rule-based BIM checking, standard GNN scoring, and TiDE without causal fusion in Figure 4. Figure 4(a) shows that the proposed method does not always choose the shortest path; a slightly longer route may be accepted when it avoids crane overlap or a temporary storage bottleneck. Figure 4(b) reports collision-risk score, where the largest reduction occurs in areas with several cranes and obstacles. Figure 4(c) shows hoisting-time reduction, indicating that the model delays only routes with strong causal evidence of hazard. Multi-metric evaluation is supported by explainability research because operational choices should be based on several observable outcomes [26].

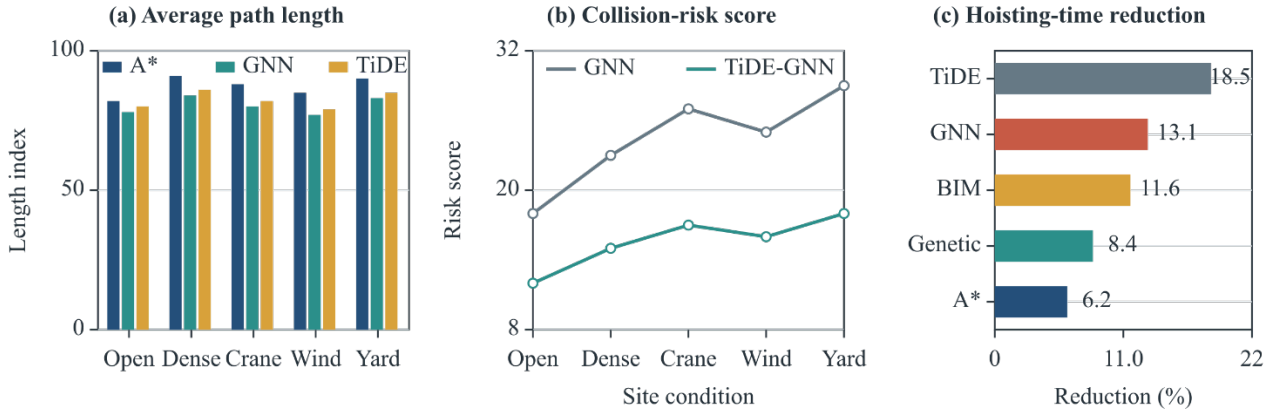


Figure 4. Path optimization performance under different site conditions. (a) Average path length. (b) Collision-risk score. (c) Hoisting-time reduction.

When compared to rule-based BIM checking, genetic planning, and standard GNN scoring, the average route cost drops by 14.8%, 11.6%, and 8.3%, respectively. The suggested model has a near-collision frequency of 5.4%, while the standard GNN score is 7.9%. The reduction is more noticeable for routes that go via temporary unloading regions; in other words, when the temporary obstacle condition immediately blocks the lifting corridor, the causal mask gives it a comparatively large weight. The basic GNN baseline underestimates the transient danger during a brief bottleneck because it tends to smooth out this evidence with nearby safe pathways. For permanent columns, walls, and crane envelopes, a rule-based BIM approach is appropriate; however, it is less responsive to alterations in the installation sequence or changes in the storage aisle caused by vehicles. Because the penalty is averaged throughout the whole path, the population search may still contain a dangerous candidate even though the genetic-planning baseline has a comparatively short competitive path length. Because graph edges record when a component enters a high-risk area and the temporal encoder assesses if the risk has been expanded, the suggested model is more sensitive to brief harmful periods. Because many crane accidents are triggered by a limited portion, a poor viewing angle, or a brief overlap with other activities rather than a long, dangerous route, this behaviour is helpful for real route evaluation. Because the planner can identify whether the alert is caused by geometry, weather, crane overlap, or schedule pressure, Barredo Arrieta et al. [27] are pertinent to the need for explainable AI in operational decision support.

The safety comparison with baseline planning methods is displayed in Figure 5. Figure 5(a) reports near-collision frequency after route selection; in obstacle-dense zones, a short-distance heuristic can produce a higher near-collision rate. Figure 5(b) reports constraint-violation ratios, including rated-load exceedance, minimum-clearance failure, forbidden-zone crossing, and crane-overlap conflict. The proposed method has a violation rate of 1.8%, compared with 3.9% for standard GNN scoring and 5.6% for A* search. The model links local route segments with global site restrictions so that conflicts appearing only during rotation or schedule overlap can be detected.

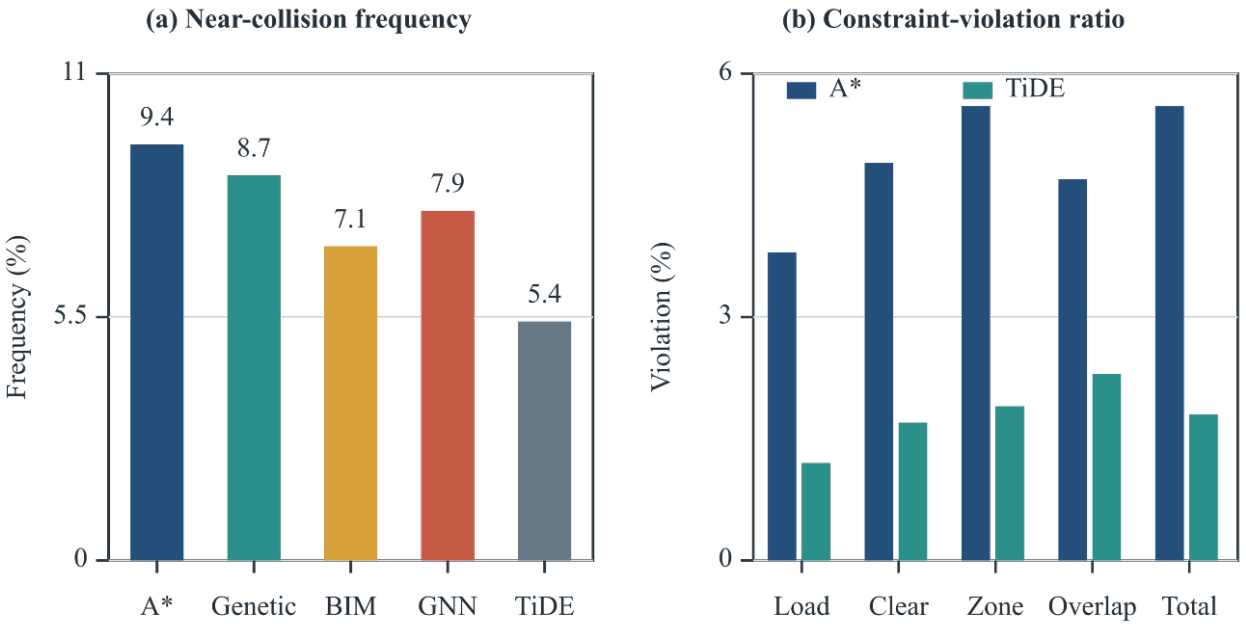


Figure 5. Safety comparison against baseline planning methods. (a) Near-collision frequency. (b) Constraint-violation ratio.

For various lift types, the models provide varying safety benefits. Since the shortest path is frequently already possible, the gain over A* search is minimal for straightforward slab lifting in open spaces. Stricter rotating clearance requirements and more sensitive load distribution result in a comparatively higher increase in size for facade panels, stair modules, and heavy beams. The second is that the route must have a comparatively significant dynamic separation since the two cranes are at the same building corner. In this situation, a planning technique that just takes into account the final path shape might not be able to identify a transient conflict. At off-peak times, it is the same. If the operator is unable to consistently monitor the component edge or final alignment, a route that satisfies the clearance criteria may nonetheless be rejected. The suggested approach decreases direct approval for visually poor pathways without rejecting all of them and gives these situations a greater review likelihood. Construction warning systems should take field-specific risk situations into account, according to research on safety-helmet detection [28]. This rule also applies to hoisting pathways, where the cost of a false safe judgement is far more than a little routing delay.

4.3. Ablation, Robustness, and Deployment Analysis

The ablation and robustness findings are displayed in Figure 6. Figure 6(a) removes causal fusion and makes the model more sensitive to storage-zone frequency, which can create false high-risk labels for familiar paths. Figure 6(b) removes graph message passing, weakening the detection of multi-hop conflicts such as vehicle blockage that later causes crane overlap. Figure 6(c) removes TiDE temporal encoding, reducing performance under changing wind windows and temporary schedule compression. Figure 6(d) adds missing obstacle updates, delayed crane telemetry, and reduced visibility. Under medium disturbance, the proposed model keeps warning accuracy above 88.4%, while regular GNN scoring drops below 83.0% [29].

The ablation study indicates that these modules serve various purposes. When a linked but indirect trait is present, causal fusion typically lowers incorrect high-risk labelling. The goal of graph message forwarding is to improve the identification of path conflicts between linked entities. Changes over time, such as the arrival of a new delivery vehicle in the yard or a rise in wind speed during a delayed lift, can be handled via temporal encoding. The quantity of reviews has also decreased due to fewer courses. The model cannot differentiate between a direct danger and a coincidental site pattern in the absence of causal fusion; hence a generic route is sent for manual review. Because the triggering evidence is dispersed among crane, obstacle, and schedule nodes, certain high-risk pathways are not detected without graph message forwarding. The model could still suggest a route that was secure ten minutes ago but is now crowded due to a material delivery if temporal encoding is not used. In order to assist site administrators, understand why a suggested path has been changed, the three modules are not simply integrated into a single model; rather, distinct forms of evidence are employed for separate models. Determining if the model has to be too simplified for edge deployment can also be aided by ablation research. To cut down on computation, a module is removed; nevertheless, this may result in more human decision-making and longer coordination times overall.

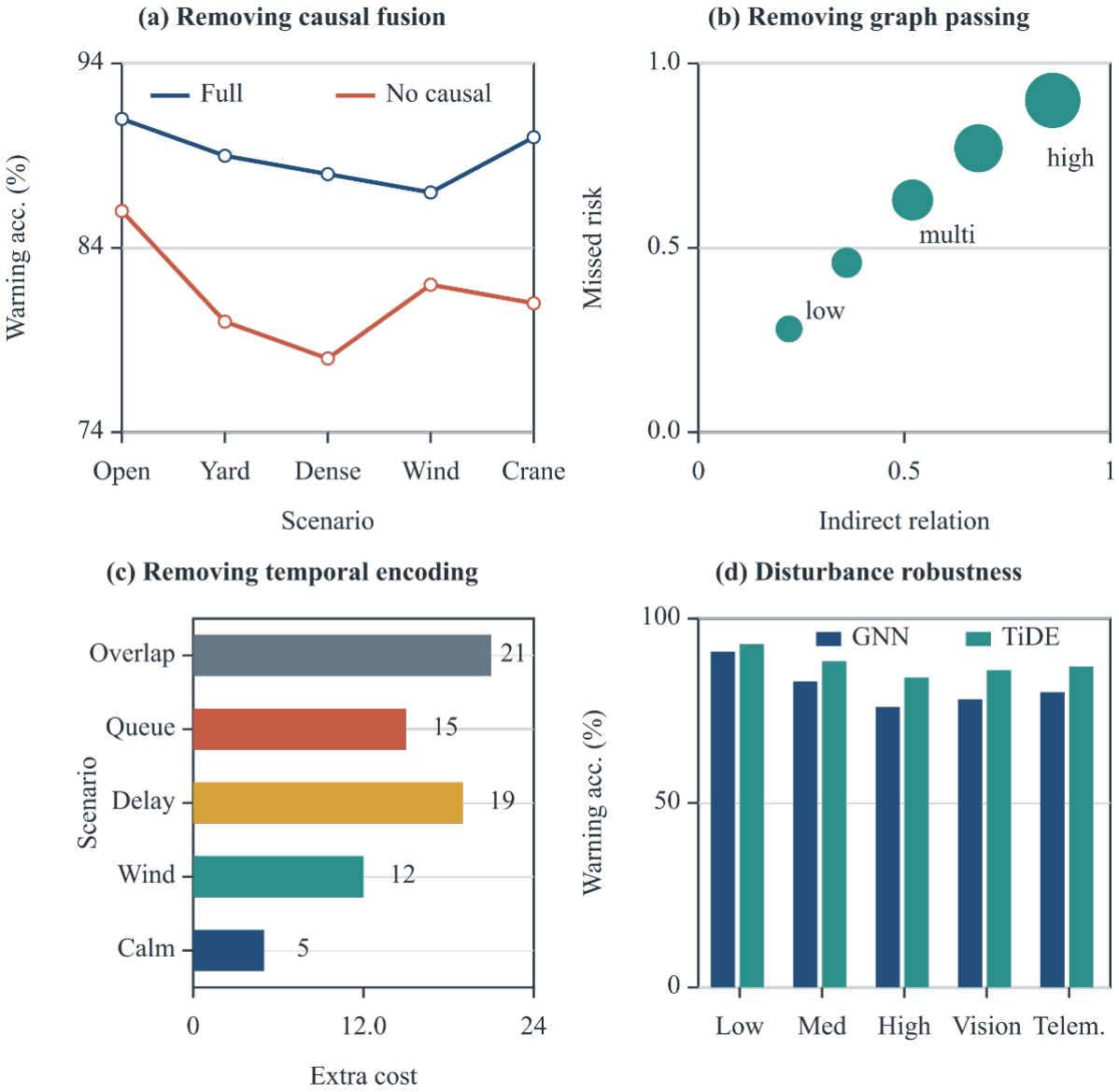


Figure 6. Ablation and robustness results of the TiDE-GNN model. (a) Removing causal fusion. (b) Removing graph message passing. (c) Removing temporal encoding. (d) Disturbance robustness.

The deployment-oriented route review results are displayed in Figure 7. Figure 7(a) reports operator review workload; the proposed model reduces manual evaluation from 28.5% to 19.3% without increasing missed high-risk cases. High-risk routes are ordered by triggering evidence rather than removed from assessment, so the operator can first inspect the primary cause. Figure 7(b) reports path update latency. Median inference time is 0.42 seconds per candidate group on a workstation and 1.18 seconds on an edge industrial computer. This remains suitable for planning-stage route comparison before the hook begins to move [30].

The remaining inaccuracies fall into three categories. First, moving equipment may enter the path after the most recent obstacle map update. Second, wind disturbance may be underestimated because local gusts between building faces can be stronger than the site weather-station reading. Third, some manually marked near-misses are inconsistent because operators use different safety margins. A review queue is therefore necessary, especially for high-consequence components moving through partially visible areas. The warning explanation tells the operator whether the route should be checked because of temporary blockage, crane overlap, weather, visibility, or schedule pressure.

5. Conclusion

A Causal-Guided Fusion TiDE-GNN model for prefabricated-component hoisting route optimization is presented in this study. The method represents components, cranes, obstacles, weather, installation targets, and scheduling states as a dynamic graph, then uses causal fusion, TiDE temporal encoding, and graph message passing to rank candidate paths. In the simulated dataset, the proposed method improves warning precision to 91.2%, lowers near-collision frequency by 31.6%, and reduces average path cost by 14.8%. The findings show that hoisting optimization should consider

geometry, temporal state, operational constraints, and causal safety evidence together rather than treating the task as a shortest-path problem.

The research remains at an early stage. The simulated dataset cannot fully reproduce sudden worker entry, missing crane telemetry, short signal loss, unrecorded material stacking, local wind gusts, or inconsistent manual near-miss labels. Some causal criteria are based on expert assumptions, simulated interventions, and historical near-miss data, so they may not capture all project-specific planning practices. Obstacle-map freshness and schedule-data quality are also important limitations. If field-management software refreshes these inputs slowly, a recommended path can become outdated before final lift approval.

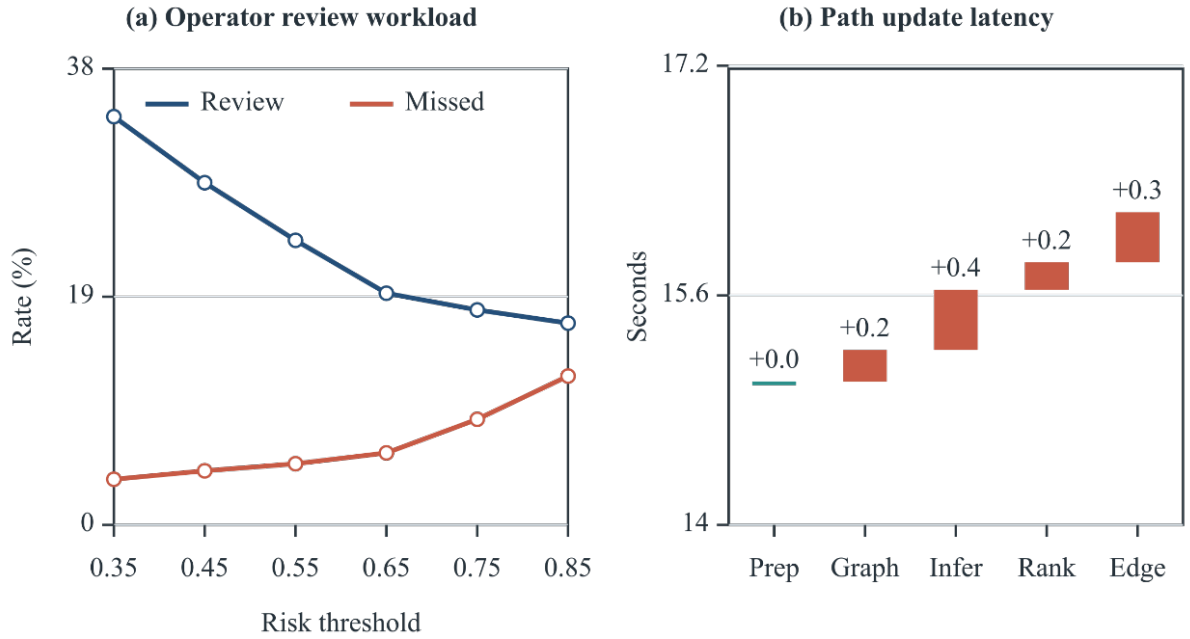


Figure 7. Deployment-oriented path review results. (a) Operator review workload. (b) Path update latency.

For field verification, real tower crane records, BIM updates, panoramic site photos, wind-field sensors, and operator input will all be integrated in the future. To ascertain whether safety parameters are genuinely connected to lift results, the model may update a causal graph using intervention data. Multi-crane cooperative optimisation, uncertainty-aware route approval, and interaction with digital-twin construction platforms will all be investigated in future research. The concept will be more useful on prefabricated construction sites thanks to the extensions.

6. Declarations

6.1. Author Contributions

Konrad Wesołowski contributes to conceptualization, methodology, software, validation, analysis, investigation, data collection, draft preparation, manuscript editing, visualization, supervision, project administration, and funding acquisition. Fabian Kołodziej contributes to validation, analysis, investigation, data collection, draft preparation. Radek Gromek contributes to software, validation. All authors have read and agreed with the manuscript before its submission and publication.

6.2. Funding and Acknowledgments

This research received no specific financial support from any funding agency.

6.3. Institutional Review Board Statement

Not applicable.

6.4. Informed Consent Statement

Not applicable.

6.5. Declaration of Competing Interest

Not applicable.

6.6. Declaration of Competing Interest

The authors declare that they have no known competing financial interests or personal relationships that could have appeared to influence the work reported in this paper.

6.7. Declaration of generative AI and AI-assisted technologies

During the preparation of this manuscript, the authors utilized Grammarly for linguistic polishing, logical organization and draft revision. The generative AI tool was not involved in research design, data collection, data analysis, or the equation of core conclusions. All outputs generated by AI were reviewed, revised and verified manually by the authors. The authors take full responsibility for all content of this manuscript.

7. References

[1] Pan, Y., & Zhang, L. (2021). Roles of artificial intelligence in construction engineering and management: A critical review and future trends. Automation in Construction, 122, 103517. https://doi.org/10.1016/j.autcon.2020.103517.

[2] Zhang, H., & Yu, L. (2021). Site layout planning for prefabricated components subject to dynamic and interactive constraints. Automation in Construction, 126, 103693. https://doi.org/10.1016/j.autcon.2021.103693.

[3] Zhu, A., Zhang, Z., & Pan, W. (2022). Crane-lift path planning for high-rise modular integrated construction through metaheuristic optimization and virtual prototyping. Automation in Construction, 141, 104434. https://doi.org/10.1016/j.autcon.2022.104434.

[4] Zhao, Y., Cao, C., & Liu, Z. (2022). A framework for prefabricated component hoisting management systems based on digital twin technology. Buildings, 12(3), 276. https://doi.org/10.3390/buildings12030276.

[5] Ji, Y., & Leite, F. (2018). Automated tower crane planning: Leveraging 4-dimensional BIM and rule-based checking. Automation in Construction, 93, 78-90. https://doi.org/10.1016/j.autcon.2018.05.003.

[6] Zhang, H., & Yu, L. (2020). Dynamic transportation planning for prefabricated component supply chain. Engineering, Construction and Architectural Management, 27(9), 2553-2576. https://doi.org/10.1108/ECAM-12-2019-0674.

[7] Xie, L., Chen, Y., & Chang, R. (2021). Scheduling optimization of prefabricated construction projects by genetic algorithm. Applied Sciences, 11(12), 5531. https://doi.org/10.3390/app11125531.

[8] George, M. R., Nalluri, M. R., & Anand, K. B. (2022). Application of ensemble machine learning for construction safety risk assessment. Journal of The Institution of Engineers (India): Series A, 103(4), 989-1003. https://doi.org/10.1007/s40030-022-00690-w.

[9] Reja, V. K., Varghese, K., & Ha, Q. P. (2022). Computer vision-based construction progress monitoring. Automation in Construction, 138, 104245. https://doi.org/10.1016/j.autcon.2022.104245.

[10] Cho, S., & Han, S. (2022). Reinforcement learning-based simulation and automation for tower crane 3D lift planning. Automation in Construction, 144, 104620. https://doi.org/10.1016/j.autcon.2022.104620.

[11] Kayhani, N., Taghaddos, H., Mousaei, A., Behzadipour, S., & Hermann, U. (2021). Heavy mobile crane lift path planning in congested modular industrial plants using a robotics approach. Automation in Construction, 122, 103508. https://doi.org/10.1016/j.autcon.2020.103508.

[12] Taghaddos, H., Hermann, U., & Abbasi, A. (2018). Automated crane planning and optimization for modular construction. Automation in Construction, 95, 219-232. https://doi.org/10.1016/j.autcon.2018.07.009.

[13] Qi, B., Costin, A., & Razkenari, M. (2022). An ontology for manufacturability and constructability of prefabricated component. Computing in Civil Engineering 2021, 745-752. https://doi.org/10.1061/9780784483893.092.

[14] Hyun, H., Yoon, I., Lee, H. S., Park, M., & Lee, J. (2021). Multiobjective optimization for modular unit production lines focusing on crew allocation and production performance. Automation in Construction, 125, 103581. https://doi.org/10.1016/j.autcon.2021.103581.

[15] Getuli, V., Capone, P., Bruttini, A., & Isaac, S. (2020). BIM-based immersive virtual reality for construction workspace planning: A safety-oriented approach. Automation in Construction, 114, 103160. https://doi.org/10.1016/j.autcon.2020.103160.

[16] Poh, C. Q. X., Ubeynarayana, C. U., & Goh, Y. M. (2018). Safety leading indicators for construction sites: A machine learning approach. Automation in Construction, 93, 375-386. https://doi.org/10.1016/j.autcon.2018.03.022.

[17] Wu, Z., Pan, S., Chen, F., Long, G., Zhang, C., & Yu, P. S. (2021). A comprehensive survey on graph neural networks. IEEE Transactions on Neural Networks and Learning Systems, 32(1), 4-24. https://doi.org/10.1109/TNNLS.2020.2978386.

[18] Zhou, J., Cui, G., Hu, S., Zhang, Z., Yang, C., Liu, Z., Wang, L., Li, C., & Sun, M. (2020). Graph neural networks: A review

of methods and applications. AI Open, 1, 57-81. https://doi.org/10.1016/j.aiopen.2021.01.001.

[19] Lim, B., & Zohren, S. (2021). Time-series forecasting with deep learning: A survey. Philosophical Transactions of the Royal Society A, 379(2194), 20200209. https://doi.org/10.1098/rsta.2020.0209.

[20] Lim, B., Arık, S. Ö., Loeff, N., & Pfister, T. (2021). Temporal fusion transformers for interpretable multi-horizon time series forecasting. International Journal of Forecasting, 37(4), 1748-1764. https://doi.org/10.1016/j.ijforecast.2021.03.012.

[21] Yu, B., Yin, H., & Zhu, Z. (2018). Spatio-temporal graph convolutional networks: A deep learning framework for traffic forecasting. Proceedings of the Twenty-Seventh International Joint Conference on Artificial Intelligence, 3634-3640. https://doi.org/10.24963/ijcai.2018/505.

[22] Wu, Z., Pan, S., Long, G., Jiang, J., & Zhang, C. (2019). Graph WaveNet for deep spatial-temporal graph modeling. Proceedings of the Twenty-Eighth International Joint Conference on Artificial Intelligence, 1907-1913. https://doi.org/10.24963/ijcai.2019/264.

[23] Yao, L., Chu, Z., Li, S., Li, Y., Gao, J., & Zhang, A. (2021). A survey on causal inference. ACM Transactions on Knowledge Discovery from Data, 15(5), Article 74. https://doi.org/10.1145/3444944.

[24] Nauta, M., Bucur, D., & Seifert, C. (2019). Causal discovery with attention-based convolutional neural networks. Machine Learning and Knowledge Extraction, 1(1), 312-340. https://doi.org/10.3390/make1010019.

[25] Ruff, L., Kauffmann, J. R., Vandermeulen, R. A., Montavon, G., Samek, W., Kloft, M., Dietterich, T. G., & Müller, K. R. (2021). A unifying review of deep and shallow anomaly detection. Proceedings of the IEEE, 109(5), 756-795. https://doi.org/10.1109/JPROC.2021.3052449.

[26] Vilone, G., & Longo, L. (2021). Notions of explainability and evaluation approaches for explainable artificial intelligence. Information Fusion, 76, 89-106. https://doi.org/10.1016/j.inffus.2021.05.009.

[27] Barredo Arrieta, A., Díaz-Rodríguez, N., Del Ser, J., Bennetot, A., Tabik, S., Barbado, A., García, S., Gil-López, S., Molina, D., Benjamins, R., Chatila, R., & Herrera, F. (2020). Explainable artificial intelligence (XAI): Concepts, taxonomies, opportunities and challenges toward responsible AI. Information Fusion, 58, 82-115. https://doi.org/10.1016/j.inffus.2019.12.012.

[28] Han, K., & Zeng, X. (2022). Deep learning-based workers safety helmet wearing detection on construction sites using multi-scale features. IEEE Access, 10, 718-729. https://doi.org/10.1109/ACCESS.2021.3138407.

[29] Hayat, A., & Morgado-Dias, F. (2022). Deep learning-based automatic safety helmet detection system for construction safety. Applied Sciences, 12(16), 8268. https://doi.org/10.3390/app12168268.

[30] Hu, S., Fang, Y., & Guo, H. (2021). A practicality and safety-oriented approach for path planning in crane lifts. Automation in Construction, 127, 103695. https://doi.org/10.1016/j.autcon.2021.103695.